



HAL
open science

Wideband high-gain transmitarray antenna for point-to-point communications at 300 GHz

Orestis Koutsos, Francesco Foglia Manzillo, Antonio Clemente, Ronan Sauleau

► To cite this version:

Orestis Koutsos, Francesco Foglia Manzillo, Antonio Clemente, Ronan Sauleau. Wideband high-gain transmitarray antenna for point-to-point communications at 300 GHz. EuMC 2021 - European Microwave Conference 2021, Apr 2022, London, United Kingdom. cea-03637083

HAL Id: cea-03637083

<https://cea.hal.science/cea-03637083>

Submitted on 11 Apr 2022

HAL is a multi-disciplinary open access archive for the deposit and dissemination of scientific research documents, whether they are published or not. The documents may come from teaching and research institutions in France or abroad, or from public or private research centers.

L'archive ouverte pluridisciplinaire **HAL**, est destinée au dépôt et à la diffusion de documents scientifiques de niveau recherche, publiés ou non, émanant des établissements d'enseignement et de recherche français ou étrangers, des laboratoires publics ou privés.

Wideband High-Gain Transmitarray Antenna for Point-to-Point Communications at 300 GHz

Orestis Koutsos^{#1}, Francesco Foglia Manzillo^{#2}, Antonio Clemente^{#3}, Ronan Sauleau^{*4}

[#]CEA-Leti, Univ. Grenoble Alpes, F-38000 Grenoble, France

^{*}Univ Rennes, CNRS, Institut d'Électronique et des Technologies du numérique (IETR) – UMR 6164, F-35000 Rennes, France

{¹orestis.koutsos, ²francesco.fogliamanzillo, ³antonio.clemente}@cea.fr, ⁴ronan.sauleau@univ-rennes1.fr

Abstract — The design and characterization of a 60×60-element high-gain, wideband transmitarray antenna at 300 GHz are presented. A numerical model is used to accurately design the 8 phase-shifting anisotropic unit-cells of the array (3-bit phase quantization). The planar lens comprises only three metal layers and no metallized vias. It is fabricated using a low-cost, standard printed circuit board technology. A 20-dBi horn is used as a feed. The experimental characterization demonstrates a peak gain of 37.0 dBi with a maximum aperture efficiency of 48.6% and a 1-dB gain bandwidth of 19.0%. These features, combined with the cost-efficient fabrication process, make the prototype a very attractive candidate for point-to-point communications in the 300-GHz band.

Keywords — transmitarray antenna, sub-THz, 300 GHz, Beyond 5G, point-to-point, high gain, printed circuit board.

I. INTRODUCTION

The continuous growth of the global mobile traffic and connected objects is leading to the saturation of the current wireless network capacity. Possible solutions could be represented by the network densification using point-to-point links, such as backhauls and fronthauls, and by the exploitation of the high end of the millimeter-wave (mmW) range. The larger absolute available bandwidth beyond 100 GHz, could enable data-rates up to 1 Tb/s [1]. Therefore, it is crucial to develop high-gain, efficient and wideband antennas using reliable and affordable technologies. However, the current sub-THz antenna solutions rely on expensive, high-resolution technologies, such as low temperature co-fired ceramic (LTCC) and silicon-on-Insulator (SOI) micromachining [2]-[5].

Transmitarrays (TA) are very attractive candidates for high-gain and wideband applications [6]-[11]. These antenna systems do not require lossy feed networks and do not suffer from feed blockage. In addition, the phase-shifting array is compatible with planar fabrication processes, such as printed circuit board (PCB) technology. However, the few PCB-based TAs demonstrated beyond 100 GHz are limited in gain and bandwidth [10] or include vias, which increase the costs and sensitivity to standard fabrication tolerances [11].

In this contribution, a 60×60-element TA antenna, realized in PCB technology, is presented for point-to-point communications at 300 GHz. The proposed unit-cell (UC) is a three-layer, vialess anisotropic structure. This architecture became quickly attractive for designing TAs thanks to its

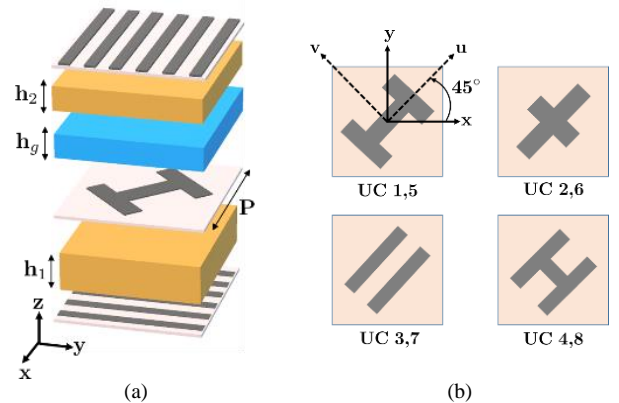


Fig. 1. (a) Exploded view of the square TA unit-cell. The three metal layers (illustrated in grey color) are interleaved by two dielectric spacers (in orange) and a bonding film (in blue). (b) Rotator patterns for the proposed 3-bit TA. A second unit-cell for each rotator design is obtained by mirroring the element with respect to the y -axis.

wideband behavior and the possibility to tune the phase of transmission varying only the geometry of the inner layer [6], [7], [10].

The design procedure of the proposed unit-cell, described in Section II, resorts to a cascaded sheet admittance model, introduced by the authors in [8]. Then in Section III, the design and characterization of the prototype is detailed. The optimal focal distance and phase distribution of the array are selected to maximize the gain and aperture efficiency, considering a 20-dBi feed illumination. The measured antenna gain (37.0 dBi) is very close to the maximum achievable theoretical value, showing the effectiveness of the UC design procedure. Finally, the prototype is compared to high-gain state-of-the-art antennas at frequencies beyond 100 GHz.

II. UNIT-CELL DESIGN AND OPTIMIZATION

A. Unit-Cell Geometry and Modelling

The stack-up of the unit-cell (UC) is shown in Fig. 1(a). The structure comprises three metal layers, interleaved by two dielectric spacers and one bonding film. Specifically, two linear polarizers are arranged orthogonally on the outer

Table I. Realized admittance values and phase of transmission at 300 GHz for the rotators of Fig. 1(b).

Unit-cell	$Im\{Y_u\}\eta_0$	$Im\{Y_v\}\eta_0$	Phase ($^\circ$)
UC 1	3.854	-0.83	58
UC 2	2.17	-1.86	90
UC 3	0.44	-4.58	140
UC 4	-0.46	-12	174
UC 5	-0.83	3.854	238
UC 6	-1.86	2.17	270
UC 7	-4.58	0.44	320
UC 8	-12	-0.46	354

surfaces, allowing almost purely x - and y -polarized waves to go through the bottom and top side, respectively. The inner layer, referred to as rotator, realizes the polarization conversion. This UC is particularly convenient for the design of broadband TAs with high-phase resolution [6]. Indeed, the rotator geometry can be modified to tune the transmitted phase without significantly affecting the 90° polarization rotation nor the insertion loss (IL).

The analysis of this structure and the design of multiple low-loss phase-shifting UCs can be eased and enhanced by using the theoretical model and sheet impedance synthesis procedure [8]. Specifically, each metal layer is modelled as a 2×2 anisotropic admittance tensor. In the xy system, due to the polarization conversion properties, the tensor associated to the rotator is non-diagonal. The transmission of the unit-cell is then calculated through a cascaded transfer matrix approach, as a function of the admittances of the layers, modelling the dielectric spacers as transmission lines. The admittance tensor of the rotator is then diagonalized so that the rotator is entirely described by a pair of admittances, namely Y_u and Y_v , in the crystal axes coordinate system (uv system in Fig. 1(b)). Thanks to this coordinate transformation, the transmission coefficient can be analytically expressed as

$$S_{21} = \pm \frac{(Y_v - Y_u)\epsilon_r\eta_0}{\epsilon_r^2 + Y_v Y_u \eta_0^2 + (Y_v - Y_u)\epsilon_r\eta_0}, \quad (1)$$

where ϵ_r is the relative permittivity of the dielectric spacers and η_0 is the impedance of free-space. The above expression is derived assuming ideal polarizers, when the overall UC thickness is half a wavelength in the dielectric and the rotator is equally spaced from the two grids. Moreover, to minimize the IL, the rotator is designed so that the crystal axes are at 45° (or 135°) with respect to the xy system. The magnitude of transmission coefficient in (1) is maximized when the rotator admittances fulfil the following relation

$$Y_u Y_v = \left(\frac{\epsilon_r}{\eta_0}\right)^2. \quad (2)$$

It can be demonstrated that the proposed UC can achieve both perfect transmission and full phase coverage. In addition, based on (2) the rotator must exhibit purely inductive and capacitive properties along the u - and v -axis, respectively.

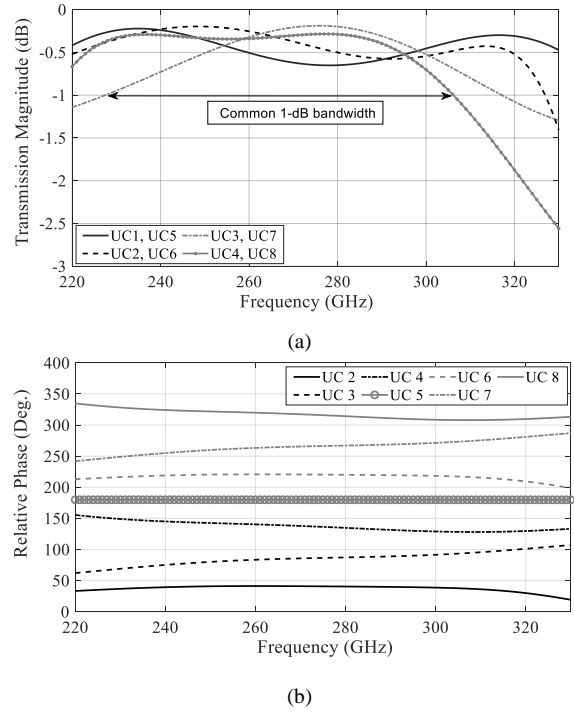


Fig. 2. Simulated transmission coefficients of the eight unit-cells. (a) Magnitude and (b) relative phase considering UC1 as a reference UC.

A relation similar to (2) can be found considering the actual polarization grids. Once the locus of optimal rotator described by (2) is found, 2^N admittance pairs (Y_u, Y_v) introducing equi-spaced phase shifts can be selected to design a TA with uniform N -bit phase quantization. In this work, a 3-bit TA design is presented to ensure low quantization loss. The optimal rotator impedances of the eight UCs are listed in Table I. They have been determined using the described procedure at 300 GHz and considering spacers of relative permittivity $\epsilon_r = 3$ and thicknesses $h_1 = h_2 = h_g = 0.127$ mm.

B. Unit-Cell Design and Results

The next design step is the physical implementation of the optimal admittances of the rotators. In this work, the rotator designs were optimized using a full-wave commercial solver (Ansys Electronic Desktop 2020) to approach the target values and ensure the technological feasibility. In order to make these designs suitable for a low-cost PCB process, the minimum conductor width and spacing were set at $80 \mu\text{m}$.

To account for these strict constraints, different rotator designs were employed, as shown in Fig. 1(b). By mirroring the rotator with respect to the y -axis, a second phase-state is found, shifted by 180° with respect to the corresponding original design. Thus, only four different rotators are needed for a 3-bit design. The periodical size of the unit-cells is $P = 0.5 \text{ mm} = 0.5\lambda_0$, where λ_0 is the free-space wavelength at 300 GHz.

The two grids are assumed identical and their width and gap are set at $80\ \mu\text{m}$ and $170\ \mu\text{m}$, respectively. Two low-loss Astra MT77 substrates ($\epsilon_r = 3$, $\tan \delta = 0.0017$) and a bonding film ($\epsilon_{rg} = 2.97$, $\tan \delta_g = 0.0019$) are used for the spacers. Therefore, the total thickness of the TA is $0.255\lambda_0$ ($0.44\lambda_0/\sqrt{\epsilon_r}$) at 300 GHz and the minimum IL, calculated using the model, is about 0.25 dB. The transmission coefficients of the 8 unit-cells, computed under normal incidence enforcing periodic boundary conditions, are shown in Fig. 2. A wideband behavior is observed with a common 1-dB bandwidth of almost 85 GHz. The relative phase shifts are very close to 45° and the phase error is less than 15° in the common bandwidth.

III. TRANSMITARRAY ANTENNA

A. Antenna Design and Optimization

The design of the TA antenna is performed with a hybrid simulation tool. An iterative procedure is used to optimize the array phase distribution for maximum gain and aperture efficiency, as a function of the focal distance. A 60×60 -element TA ($30 \times 30 \lambda_0^2$) is designed, in order to achieve a gain higher than 35 dBi.

The main drawback for large TAs optimized at a single frequency, is the narrowband performance due to the frequency-dependent spatial phase delay [9]. This effect can be partly compensated by changing the properties of the illumination. In a single-feed architecture, the bandwidth can be improved by increasing the directivity of the focal source, at the expense of an increased focal distance. Nevertheless, at sub-THz frequencies the antenna height remains relatively small. Therefore, a 20-dBi horn (model 32240-20 by Flann Microwave) was selected as a good trade-off between antenna profile and bandwidth coverage. The optimal focal distance is $F = 55\ \text{mm}$, corresponding to a focal-to-diameter ratio $F/D = 1.83$ and an edge taper of 13 dB, when the frequency of optimization is set at 280 GHz.

As a comparison, when a 10-dBi source is considered, the distance maximizing the gain at the same frequency is $F = 20\ \text{mm}$ ($F/D = 0.67$) and the edge taper is 17 dB. However, the simulated 1-dB gain bandwidth becomes about 7.0%, whereas in the proposed design it is close to 20.0%. With the 10-dBi horn, the simulated maximum aperture efficiency (48.6%) is also smaller if compared to the 20-dBi illumination (59.3%).

B. Measurements

The antenna prototype, shown in Fig. 3, was measured in the CEA-Leti far-field anechoic chamber. The gain is plotted as a function of frequency in Fig. 4. The measured peak gain is 37.0 dBi at 290.9 GHz, with an aperture efficiency of 47.2%. The maximum aperture efficiency is 48.6% at 279.4 GHz, which is close to the optimization frequency, and it is more than 40.0% between 250 and 300 GHz. The measured 1-dB gain bandwidth is approximately 56 GHz, from 264 to 320 GHz, which is about 19.0%. The good agreement between simulations and measurements validates the design approach. Table II compares the peak gain and aperture efficiency

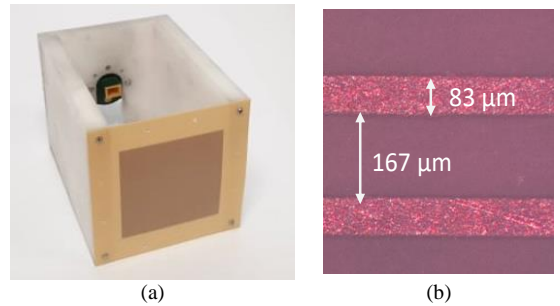


Fig. 3. (a) Photograph of the TA antenna prototype and (b) image of one of the polarizers.

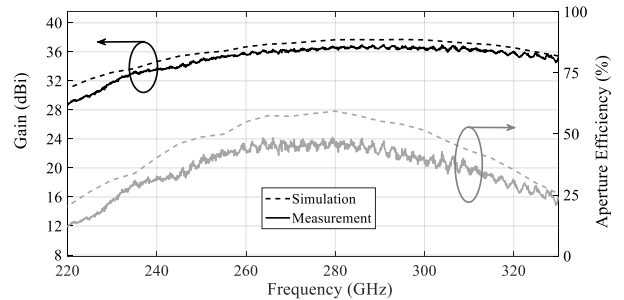


Fig. 4. Gain and aperture efficiency of the antenna prototype as a function of frequency. Dashed line: simulation. Solid line: measurement.

Table II. Peak gain and aperture efficiency at 280 GHz of the prototype compared to the upper bounds (Ideal TA) and the values achievable using the optimal admittances of Table I.

Scenario	Gain (dBi)	Aperture eff. (%)
Ideal TA	38.4	66.0
Optimal 3-bit	38.0	60.7
Designed 3-bit	37.7	59.3
Measured	37.0	48.6

achieved by the 3-bit designed TA at 280 GHz to the values computed for two reference designs with the same size and illumination. The measured gain is only 1.4 dB lower than the value that could be reached using an ideal TA, i.e. a reflectionless lens providing perfect phase compensation. The gain of the optimal 3-bit TA design is estimated assuming the optimal rotator admittances in Table I for the computation of the transmission coefficients of the eight unit-cells. It is only 1 dB higher than the gain computed considering the actual UCs, validating the design of the rotators described in Section II.B.

The shape of the beam is very stable across the frequency range, as shown in Fig. 5. The half-power beamwidth (HPBW) is approximately 2° in the 1-dB gain bandwidth, in both principal planes. The radiation pattern at two frequency points is shown in Fig. 6. The first sidelobe level is about -24.6 dB and -25.8 dB in the H- and E-plane, respectively. A sidelobe level discrepancy between simulation and measurements is observed in the H-plane (Fig. 6(a)), probably caused by the impact of the mechanical support that is placed in this side of the antenna, as shown in Fig. 3(a). The cross-polarization discrimination is greater than -26.0 dB across the entire band.

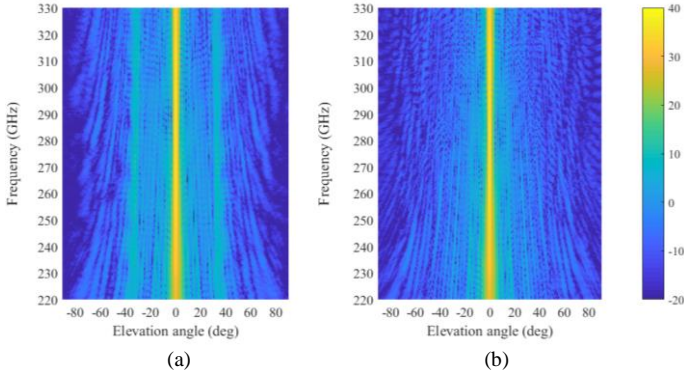


Fig. 5. Measured beam shape as a function of the elevation angle and the frequency in two cut-planes. (a) H-plane, (b) E-plane.

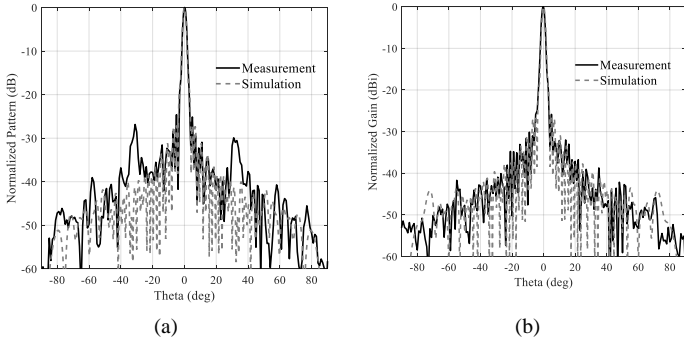


Fig. 6. Simulated and measured radiation pattern of the TA. (a) H-plane at 300GHz, (b) E-plane at 300GHz.

The prototype features and measured performance are compared to state-of-the-art (SotA), large aperture antennas at sub-THz frequencies in Table III. It achieves both wideband and efficient characteristics, while the radiation is very stable across the entire bandwidth. Even with a low-cost fabrication process, the antenna performance is comparable to prototypes leveraging more expensive high-resolution technologies, such as silicon micromachining [3], [5] and quartz lithography [4].

IV. CONCLUSION

A wideband, efficient large aperture TA antenna for point-to-point communications at 300 GHz was presented. A theoretical model was employed to study and effectively design three-layer and vialess unit-cells. A 3-bit $30 \times 30 \lambda_0^2$ TA prototype was fabricated using a low-cost standard PCB technology, mounted on a 20-dBi horn. The measured peak gain and aperture efficiency are 37.0 dBi and 48.6%, respectively. The relative 1-dB and 3-dB gain bandwidth are about 19.0% and 34.0%, respectively. These results demonstrate the suitability of PCB-based TAs for high-efficiency sub-THz wireless links.

Table III. Comparison with state-of-the-art, high-gain sub-THz antennas.

Reference	This work	[2]	[3]	[4]	[5]
Freq. (GHz)	300	140	360	390	180
Architecture	TA	TA	Waveguide array	RA	Lens
Technology	PCB	LTCC	SOI micro-machining	Quartz wafer	Silicon
Aperture size (λ^2)	30×30	18.7×18.7	26.4×26.4	$\pi(12.9 \times 12.9)$	$\pi(9 \times 9)$
F/D	1.83	1.87	-	1.07	~ 1
Peak gain (dBi)	37.0	33.4	38.0	33.6	34.0
Aperture efficiency	48.6%	50.1%	64.0%	29.3%	$> 75.0\%$
1-dB Gain bandwidth	19.0%	10.7%	-	-	-
3-dB Gain bandwidth	34.0%	24.4%	22.0%	16.0%	35.0%
Sidelobe level (dB)	-24.6	-21.0	-13.0	-17.8	-15

ACKNOWLEDGMENT

This work was partly supported by the National Research Agency (ANR) through the project "Next5G" under Grant ANR 18-CEA 25-0009-01.

REFERENCES

- [1] S. Rappaport *et al.*, "Wireless communications and applications above 100 GHz: opportunities and challenges for 6G and beyond," in *IEEE Access*, vol. 7, pp. 78729-78757, 2019.
- [2] Z. Miao *et al.*, "140 GHz high-gain LTCC-integrated transmit-array antenna using a wideband SIW aperture-coupling phase delay structure," *IEEE Trans. Antennas Propag.*, vol. 66, no. 1, pp. 182-190, Jan. 2018.
- [3] A. Gomez-Torrent *et al.*, "A 38 dB gain, low-loss, flat array antenna for 320-400 GHz enabled by silicon-on-insulator micromachining," *IEEE Trans. Antennas Propag.*, vol. 68, no. 6, pp. 4450-4458, June 2020.
- [4] Z. Miao *et al.*, "A 400-GHz high-gain quartz-based single layered folded reflectarray antenna for Terahertz applications," *IEEE Trans. Terahertz Sci. Technol.*, vol. 9, no. 1, pp. 78-88, Jan. 2019.
- [5] M. A. Campo *et al.*, "Wideband circularly polarized antenna with in-lens polarizer for high-speed communications," *IEEE Trans. Antennas Propag.*, vol. 69, no. 1, pp. 43-54, Jan. 2021.
- [6] P. Feng, S. Qu and S. Yang, "Octave bandwidth transmitarrays with a flat gain," *IEEE Trans. Antennas Propag.*, vol. 66, no. 10, pp. 5231-5238, Oct. 2018.
- [7] Y. Ge, C. Lin and Y. Liu, "Broadband folded transmitarray antenna based on an ultrathin transmission polarizer," *IEEE Trans. Antennas Propag.*, vol. 66, no. 11, pp. 5974-5981, Nov. 2018.
- [8] O. Koutsos, F. Foglia Manzillo, A. Clemente and R. Sauleau, "Analysis and efficient design of sub-THz transmitarrays with three anisotropic layers," in *Proc. 15th Eur. Conf. Antennas Propag. (EuCAP)*, Dusseldorf, Germany, Mar. 2021, pp. 1-5.
- [9] F. Diaby *et al.*, "Impact of phase compensation method on transmitarray performance," in *Proc. 11th Eur. Conf. Antennas Propag. (EuCAP)*, Paris, France, Mar. 2017, pp. 3114-3118.
- [10] K. Medrar *et al.*, "H-band substrate-integrated discrete lens antenna for high data rate communication systems," *IEEE Trans. Antennas Propag. (Early Access)*, Dec. 2020.
- [11] F. Foglia Manzillo *et al.*, "Low-cost, high-gain antenna module integrating a CMOS frequency multiplier driver for communications at D-band," in *Proc. IEEE Radio Freq. Int. Circ. Symp. (RFIC)*, Boston, USA, June 2019, pp. 19-22.